Changes in the Fatty Acid Amide Levels and the Expression of Three Insect Arylalkylamine-*N*-acyltransferases in the Different Life Stages of *Bombyx mori*.

Ryan L. Anderson[1,2], Dylan J. Wallis[1,3], Suzeeta Bhandari[1], Alexandria C. Musick[1], Sydney Innes[1], and David J. Merkler[1,*]

[1]Department of Chemistry, University of South Florida, Tampa, Florida, 33620

[2]Current Address
AB Sciex, LLC
500 Old Connecticut Path
Framingham, MA 01701
E-mail: Ryan.Anderson@sciex.com

[3]Current Address
Bioinformatics Research Center
Department of Biological Sciences
North Carolina State University
1 Lampe Dr.
Raleigh, NC, 27607
E-mail: djwallis@ncsu.edu

*Corresponding Author
Dr. David J. Merkler,
Department of Chemistry
University of South Florida
4202 E. Fowler Ave., CHE 205
Tampa, FL 33620 USA
Phone: 813-974-3579
FAX: 813-974-3203
E-mail: merkler@usf.edu

Abstract

The goal of the project detailed herein is to track changes in transcript levels of three insect arylalkylamine-N-acyltransferases (iAANATs) during the life cycle of the domesticated silkworm (Bombyx mori). The purpose being to uncover key differences in the expression of these iAANATs at different life stages of the insect. Furthermore, knowing these enzymes are capable of biosynthesizing specific fatty acid amides in vitro, we wanted to characterize and quantify a panel of such lipids via liquid chromatography time-of-flight mass spectrometry (LC-QToF-MS) from purified lipid extracts of each stage of B. mori life. Our results show differences in expression for these separate iAANATs as well as a panel of fatty acid amides at different time points in the life cycle of the silkworm. The combination of iAANAT expression and fatty acid amide data provide insight on how the fatty acid amides are being synthesized in vivo.

Keywords: Arylalkylamine-*N*-acyltransferase, fatty acid amide biosynthesis, *Bombyx mori*, dopamine, serotonin

Abbreviations

Bm-iAANAT – *Bombyx mori* insect arylalkylamine *N*-acyltransferase
CoA – coenzyme A thioester
C_T = cycle threshold
PalmGly – *N*-palmitoylglycine
PalmDop – *N*-palmitoyldopamine

PalmSer – *N*-Palmitoylserotonin
Palmle – Palmitoleamide
Palm – Palmitamide
OleGly – *N*-oleoylglycine
OleEth – *N*-oleoylethanolamine
OleDop – *N*-oleoyldopamine
OleSer – *N*-oleoylserotonin
OleTrp – *N*-oleoyltryptamine
Ole – Oleamide
AracSer – *N*-arachidonoylserotonin
LinGly – *N*-linoleoylglycine
Lino – Linoleamide
SteSer – *N*-stearoylserotonin

1. Introduction

Humans and silkworms, *Bombyx mori* (*B. mori*), have a relationship that dates back approximately 5,000 years when humans first realized silk was a component of their cocoon [1]. Silk produced by the *B. mori* is now the basis of a multi-billion-dollar industry [2] that employs millions of people [3]. In addition to the economic impact of *B. mori*-generated silk, *B. mori* is a valuable model system for human disease [4-7], a useful host for the heterologous production of recombinant proteins [7-9], and could serve as a nutritious food source [10,11].

Fatty acid amides are a family of lipids found in both vertebrates and invertebrates [12-15]. Structurally, the fatty acid amides are relatively simple, R-CO-NH-R', with the acyl moiety (R-CO-) derived from fatty acids and the amine moiety (R'-NH-) derived from the biogenic amines. Subclasses of the fatty acid amide family are defined by the biogenic amine, which include the *N*-acylethanolamines (NAEs, R-CO-NH-CH_2-CH_2-OH), *N*-fatty acylglycines (NAGs, R-CH-NH-CH_2-COOH), and primary fatty acid amides (PFAMs, R-CO-NH_2). Greater than 70 different endogenous fatty acid amides have been identified from living systems with only a few having defined cellular functions [15]. In mammals, *N*-arachidonoylethanolamine (anandamide) is the endogenous ligand for cannabinoid receptors (CB_1 and CB_2) [16,17], *N*-palmitoylethanolamine is a PPAR-α agonist and may also bind to GPR55 (an orphan GPCR) [18], and oleamide regulates the sleep/wake cycle [19]. In insects, volicitin and other structurally related *N*-fatty acyl amino acid conjugates elicit the release of plant volatiles that attract predators against the insects feeding on the plant [20,21]. The known functions of anandamide, *N*-palmitoylethanolamine, oleamide, and volicitin coupled to the relatively low cellular concentrations of the fatty acid amides [22-24] have led to the consensus that the fatty acid amides are cell signaling molecules.

Volicitin and the other *N*-fatty acyl amino acid conjugates are not the only fatty acid amides produced by insects. *Amblyomma americanum* [25], *Drosophila melanogaster* [26,27], and *Bombyx mori* [28] are known to produce fatty acid amides, but their function in these insects is unclear. Not only are the functions for most of the fatty acid amides unclear, but the reactions leading to their production in the cell are similarly unclear. With the exception of the NAEs, which are produced *in vivo* from membrane phospholipids [12,18,29], pathway(s) for the biosynthesis of the other fatty acid amide subclasses are not completely defined.

We proposed an undiscovered *N*-acyltransferase produced the fatty acid amides *in vivo* [30]. Such enzymes would catalyze a reaction between a fatty acyl-CoA thioester and an amine to generate the corresponding fatty acid amide and coenzyme A (Figure 1) and, most likely, would be members of the GCN5-related superfamily of *N*-acetyltransferases (GNAT) [31,32]. Since our original hypothesis in 1996, we have identified and characterized two novel insect arylalkylamine *N*-acyltransferases (iAANATs), one from *Drosophila melanogaster* [33] and one from *Bombyx mori* [28], that utilize long-chain fatty acyl-CoA thioesters as substrates to yield fatty acid amides *in vitro*. Subsequent, expression knockdown experiments provide evidence these enzymes do function *in vivo* in fatty acid amide biosynthesis in *D. melanogaster* [34]. Gaps remain in our knowledge of the fatty acid amides despite the wealth of data on the existence of these lipids in different living systems and the work to define routes for their production *in vivo*. The fatty acid amide knowledge gap is greatest in the insects because insects do not express cannabinoid receptors [35] and often express multiple iAANATs with overlapping substrate specificities [36, 37].

To help resolve these knowledge gaps, we now report the presence and relative concentration of specific fatty acid amides across the life cycle stages of *B. mori* and couple these data to the transcript levels of the three known iAANATs expressed by *B. mori*, *Bm*-iAANAT, *Bm*-iAANAT2, and *Bm*-iAANAT3 [38-40]. We find the fatty acid amide and *Bm*-iAANAT transcript levels to be different at the different life cycle stages of the silkworm. No single fatty acid amide is found in all cycle stages and these lipid amides are most abundant in instar 3 and instar 4.

Our data reinforce the suggestion fatty acid amides are cell-signaling lipids. Each of the three *Bm*-iAANATs exhibit differences in the transcriptional expression patterns in the various life cycle stages of *B. mori*. In sum, these data suggest *Bm*-iAANAT3 does not have a role in fatty acid amide biosynthesis and the function of this

enzyme is to catalyze amine *N*-acetylation in instar 1. Unlike *Bm*-iAANAT3, *Bm*-iAANAT and *Bm*-iAANAT2 probably do have a role in fatty acid amide biosynthesis *in vivo* and also catalyze other *N*-acylation reactions important to *B. mori* in each of the life cycle stages. Our work establishes an important set of baseline data for future experiments to examine the function(s) of specific fatty acid amides and to evaluate the changes in the amidome after genetic manipulation of a specific *Bm*-iAANAT.

2. Materials and Methods

2.1 Materials

Unless otherwise stated, all reagents were of the highest quality available from reputable, commercial suppliers. *N*-Palmitoyldopamine and all other internal standards were purchased from Cayman Chemical.

2.2 Rearing of the Silkworms and Sample Collection

Bombyx mori eggs were purchased from Carolina Biological, immediately placed into a petri dish upon arrival, and fed Silkworm Artificial Dry Diet (Carolina Biological) after hatching. The different instars were identified based on the number of molts, such that the first instar (instar 1) was collected before the first molt and the fifth instar (instar 5) was collected after the fourth molt. Also, the pupae and moth life stages were collected, respectively. After collection, each sample type was immediately flash frozen in liquid N_2 and stored at -80°C before continuing any extraction of either the nucleic acids or the fatty acid amides. The pre-instar "ant" stage was not assessed because of the inconsistency in timing of the transition to instar 1.

2.3 Extraction/ Isolation of mRNA and gDNA Decontamination

Total RNA was extracted from the whole organism at the indicated life stage using TRIzol® reagent and collected using the PureLink RNA Mini Kit® from Thermo Fisher. The mRNA was obtained from the total RNA using the PolyATtract® mRNA Isolation Systems III from Promega. After the elution of mRNA in nuclease-free water, a 10 kDa centrifugal filter was used to concentrate the transcripts (15 min at 12,000 × g). A Nanodrop® (Thermo Fisher) was used to determine the final concentration of the resulting mRNA. DNase I (Thermo Fisher) was employed for the removal of genomic DNA (gDNA) and modifications made to the manufacturer's protocol for full gDNA decontamination (Table 1). The mRNA was incubated with DNase I in DNase I buffer with $MgCl_2$, and nuclease-free water at 37°C for 45 minutes, at which time 2 µL of EDTA was added while raising the temperature to 65°C for 10 minutes to inactivate the DNase I. After the completion of gDNA decontamination, the mRNA solution was diluted with nuclease-free water to a final concentration of 10 ng/µL.

2.4 One-Step RT-qPCR of Tua1, *Bm*-iAANAT, *Bm*-iAANAT2, and *B*m-iAANAT3

Separate, triplicate wells of a 96-well plate were initially loaded with 10 µL Power Up™ SYBR® Green Master Mix from Thermo Fisher, 30 ng of mRNA from a specific *B. mori* life stage and 2 µL (20 U/µL) MMLV-RT from Promega. Next, the appropriate primers were added to the wells, an essential step to delineate which amplicon was replicated. The forward and reverse primers for each amplicon type were designed to create 75-150 bp products and the primer sequences are listed in Table 2. α-Tubulin (Tua1) was chosen as the positive, endogenous control for all RT-qPCR experiments because this protein is abundantly expressed in every post-embryonic life stage of the organism [41]. In multiple quantitative studies, Tua1 was identified as a stable gene in normal tissues [42, 43] and, since the RT-qPCR was carried using mRNA isolated from whole body extracts, tissue wise variation of the gene would not be an issue at different life stages of *B. mori*. Forward and reverse primers for *B. mori* Tua1 (both at 200 nM) were added to wells A1-A3; forward and reverse primers for *Bm*-iAANAT (both at 200 nM) were added to wells B1-B3, and forward and reverse primers *Bm*-iAANAT2 (both at 200 mM) were added to wells C1-C3. Forward and reverse primers for *Bm*-iAANAT (both at 50 nM) were added to wells D1-D3. Sufficient nuclease-free water was added to each well to bring the final volume to 20 µL. A negative control substituting MMLV-RT for nuclease-free water was used to ensure total decontamination of gDNA. Another negative control substituting the mRNA template for nuclease-free water was run to ensure fluorescence was not being detected from primer-dimer formation. This entire plate-loading process was repeated separately, using mRNA from a different life stage each time. Each prepared plate was capped and briefly centrifuged before placement into an Applied Biosystems QuantStudio3 qPCR thermal cycler. The one-step RT-qPCR conditions were as follows: The reverse transcriptase phase was completed by holding the temperature at 50°C for 45 minutes and then raising the temperature to 95°C for 10 minutes to inactivate the MMLV-RT. The PCR cycles began immediately after MMLV-RT inactivation with an initial temperature hold at 95°C for 15 seconds, then lowered to 60°C for 1 minute, before returning to 95°C. This was repeated for a total of 40 cycles.

Melt curve analysis was employed after the completion of thermal cycling with holds at 95°C for 15 seconds, 60°C for 1 minute, and a final 95°C for 1 second. The cDNA products of the same amplicon were added together to

make a final volume of 40 µL and mixed with 10 µL purple loading dye from New England Biolabs (NEB). This was done for each amplicon separately, the Tua1, *Bm*-iAANAT, *Bm*-iAANAT2, and *Bm*-iAANAT3 amplicons. The resulting 50 µL PCR product mixtures and a 100 bp ladder from NEB were loaded into separate lanes of a 1.8% agarose gel containing ethidium bromide and electrophoretic separation was affected at 50 V for 90 minutes. All bands denoting significant cDNA products were extracted using the Wizard® SV Gel and PCR Clean-Up System from Promega and sequenced commercially by Eurofins Genomics.

2.5 Analysis of the RT-qPCR Data

The cycle threshold value (C_T) is the number of cycles of RT-PCR amplification required to generate the desired PCR product beyond a specific target, call the threshold [44].

The C_T values reflect transcription levels of a single product because the amplicon sequences match the sequence of the desired products and the negative control wells showed no amplification. The change in abundance for each iAANAT transcript relative to Tua1 transcript from each instar, yields the ΔC_T value ($C_{T,iAANAT} - C_{T,Tua1}$).

2.6 Extraction and Purification of Fatty Acid Amides from Different *B. mori* Life Stages

Samples of 0.5-1.0 g, depending on the life stage of a *Bombyx mori* larval instar, pupae, or moth was collected in triplicate (1.5-3.0 g total) using the sample collection method described above. To extract the fatty acid amides, the insects were first placed into a mortar and pestle with 20.8 mL of methanol per gram of solid tissue used. The remaining extraction solvents and steps, as well as the silica and Zip Tip purification protocols are described in Anderson *et al*. [28]. Blanks using the same proportionate volumes of solvents, but containing no tissue, were prepared and treated in the exact same manner as each different extraction.

2.7 LC-QTof-MS Analysis of Fatty Acid Amides from *Bombyx mori*

A 90 µL aliquot of fatty acid amide extract (eluted from the Zip Tip in acetonitrile:water, 95:5) was placed in a LC vial with glass insert and 10 µL of internal standard solution,containing 1 pmole/µL each of *N*-arachidonoylglycine d_8,
N-arachidonoylethanolamine d_8, *N*-arachidonoyldopamine d_8, and *N*-oleoylserotonin d_{17}. This was repeated for the extraction blanks, as well. Each internal standard was quantified using standard curves generated from pure compound ranging from 0.1 – 10 pmoles and each exhibiting an R^2 value of at least 0.990. Each of the deuterated internal standards were checked for, and found to be free of, any of the corresponding unlabeled compound. *Bombyx mori* lipid extracts were injected on an Agilent 6540 liquid chromatography/quadrupole time-of-flight mass spectrometer (LC-QTOF-MS) in the positive ion mode with a Kinetex 2.6 µm C_{18} 100 Å (50 × 2.1 mm) column. Analytes were separated using a gradient mixture of two solutions: mobile phase A was 0.1% (v/v) formic acid in water, while mobile phase B was 0.1% (v/v) formic acid in acetonitrile. A linear gradient of 10% mobile phase B increased to 100% B over 5 minutes, followed by a hold of 3 minutes at 100% B for the analysis of the product (flow rate of 0.6 mL/min). Post-analysis equilibration of the column was carried out with 10% mobile phase B for 10 minutes before the next injection. Through washing of the column between injections used the same solvent gradient, but at a flow rate of 1.0 mL/min. The fatty acid amides in each extraction were identified by comparison to synthetic standards with regards to retention time and *m/z* value.

Quantification of the fatty acid amides identified in the *B. mori* extracts was calculated by integrating the area under the chromatographic peak and comparing that value against standard curves prepared using the exact fatty acid amide standard. These values were normalized based on the recovery of the internal standards spiked into each solution. Finally, the pmoles were divided by the mass of starting tissue to provide the final value as pmole/g.

3. Results and Discussion

3.1 Transcript Levels for *Bm*-iAANAT, *Bm*-iAANAT2, and *Bm*-iAANAT3 at Different Life Cycle Stages of *B. mori*

Meng *et al*. [6] highlight the advantages of *B. mori* as a model organism: progeny size, short generation times, and a well-defined life cycle. The *B. mori* life cycle includes pupae, moth, and five instars, instars 1-4 defined by a molt as well as a pre-instar, "ant" stage [6]. The average of three replicates for the cycle threshold values (C_T) of three *B. mori* iAANAT amplicons, *Bm*-iAANAT, *Bm*-iAANAT2, and *Bm*-iAANAT3, and the same for the Tua1 control amplicon at the different life cycle stages are compiled in Table S1 (Supplementary Materials). The ΔC_T values data convey the change in abundance of each iAANAT transcript relative to the change in abundance of the α-tubulin (Table 3). The ΔC_T values reveal that the transcript levels of all three *Bm*-iAANATs are lower than the levels of the Tua1 at every life stage. Also, the ΔC_T values show that the expression levels of *Bm*-iAANAT ≥ *Bm*-iAANAT2 > *Bm*-iAANAT3, the exception being that the transcript levels of *Bm*-iAANAT ≈ *Bm*-iAANAT2 in instar 1 and instar 2.

For each *B. mori* iAANAT, we calculated the $\Delta\Delta C_T$ values relative to value of the value from instar 1 for each enzyme, $\Delta\Delta C_T = \Delta C_{T,instar} - \Delta C_{T,life\ stage}$. The fold changes for *Bm*-iAANAT, *Bm*-iAANAT2, and *Bm*-iAANAT3 during each life cycle stage are, thus, relative to instar 1. The fold changes were calculated using the formula, $2^{-\Delta\Delta CT}$, and are shown in Figure 2. The iAANATs serve a multitude of roles in *B. mori* and other insects [37,45], including the regulation of melanism [39,46], photoperiodism [47], cuticle sclerotization [39], amine inactivation [36], and fatty acid amide biosynthesis [34]. Insects often express a set of iAANAT isozymes [36,37], which seems related to the multitude of cellular functions attributed to these enzymes. One consequence of the metabolic importance of the iAANATs might be the constitutive expression of at least one iAANAT isozyme across the life stages of an insect as a "general purpose" iAANAT to ensure coverage for all of the iAANAT-related functions. Consistent with this hypothesis, we found only relatively small changes in the transcript levels of *Bm*-iAANAT for each stage in the life cycle of *B. mori* (Figure 2). *In vitro* substrate specific studies of *Bm*-iAANAT reveal this enzyme will accept a broad range of both acyl-CoA and amine substrates [28,38], again, consistent with the hypothesis that a "general purpose" iAANAT would be expressed at appreciable levels throughout the silkworm life cycle. Mutations in *Bm*-iAANAT exhibit aberrations in pigmentation, consistent with an *in vivo* role for the enzyme in dopamine acetylation [46,48].

In contrast, the *Bm*-iAANAT3 transcript is most abundant in instar 1 followed by a consistent decrease in the transcript level of approximately 2-fold, $\Delta\Delta C_T \sim -1.0$, in all the other life stages of *B. mori* (Figure 2). This result suggests *Bm*-iAANAT3 is most important in the first few days in the life of *B. mori*. Instar 1 lasts 3-4 days, covering the period for which the larvae emerge from the eggs as 3-4 mm darkly colored "ants", which lighten in color, molt, and approximately double in size [49]. *Bm*-iAANAT3 prefers short-chain acyl-CoA substrates [40] and catalyzes the acetyl-CoA-dependent formation of *N*-acetyldopamine, a reaction that contributes to both lightening of the *B. mori* and cuticle sclerotization. In particular, cuticle sclerotization of the mandible is essential in the first few days of life to enable the *B. mori* larvae to chew their food [50].

Our data on the transcript levels of *Bm*-iAANAT2 is similar, but not identical to the data on the transcript levels for both *Bm*-iAANAT and *Bm*-iAANAT3. Like the data for *Bm*-iAANAT, the transcript levels for *Bm*-iAANAT2 are found across all the life cycle stages. However, like the data for *Bm*-iAANAT3, *Bm*-iAANAT2 transcript levels are higher (and approximately the same) at specific life cycle stages, instar 1 and instar 5. The *Bm*-iAANAT2 transcript levels are approximately 1.7-fold, $\Delta\Delta C_T \sim -0.8$, in all the life cycle stages relative to the levels at instar 1 and instar 5 (Figure 2). The substrate specificity of *Bm*-iAANAT2 has not been defined, other than demonstrating the enzyme catalyzes the formation of *N*-acetyltryptamine from acetyl-CoA and tryptamine *in vitro* [39]. *B. mori* deficient in *Bm*-iAANAT2 show higher levels of dopamine and are darker in color [39], suggesting that *Bm*-iAANAT2 will catalyze *N*-acetyldopamine production, as well. The larval growth during instar 5 is significant. From day 1 to day 7 in instar 5, the larval weight approximately triples and larval length approximately doubles [51]. Such increases in weight and length require a rapid synthesis and sclerotization of the *B. mori* cuticle. The relatively high transcript levels of *Bm*-iAANAT2 in instar 5 suggest this enzyme functions in cuticle sclerotization. Other enzymes involved in cuticle sclerotization, dopa decarboxylase [52] and dopachrome conversion enzyme [53], are also expressed at relatively high levels in instar 5.

Often the iAANATs produced in an insect exhibit overlapping substrate specificities, rendering it difficult to attribute a specific cellular function to a specific iAANAT. In *B. mori*, the three known iAANATs catalyze *N*-acetyldopamine formation. Mutants deficient in *Bm*-iAANAT or *Bm*-iAANAT2 are viable, progress to moths, exhibit higher than wildtype levels of dopamine, and exhibit darker than wildtype coloration patterns [39,46,48]. In sum, these data suggest *Bm*-iAANAT, *Bm*-iAANAT2, and *Bm*-iAANAT3 have a role melanism and sclerotization. It could be that the cellular functions fulfilled by the iAANATs are important enough in insects that the multiplicity of isozymes guarantees at least one of the enzymes will provide sufficient function for survival, where one iAANAT serves a "back-up" to the other iAANATs. The iAANAT isozymes could exhibit different patterns of regulation not only by the binding of allosteric ligands, but also by differences in post-translational modification. Differences in tissue expression patterns at various instars for *Bm*-iAANAT and *Bm*-iAANAT2 are known [39,46], providing another potential explanation for the family of iAANATs found in insects. Lastly, definitive conclusions about the cellular roles of iAANATs cannot be based solely on transcript abundance data because transcript abundance does not perfectly correlate with either protein abundance or extent of *in vivo* enzyme activity [54]. More research is necessary to define the roles served by the iAANATs in *B. mori* and other insects.

3.2 Fatty Acid Amide Levels at Different Life Cycle Stages of *B. mori*

Total ion chromatograms (TIC) from all *B. mori* purified extracts were searched for *m/z* values and retention times matching those for the pure, fatty acid amide standards.

A match was scored positive for a metabolite when its retention time was within ± 0.2 minutes and its *m/z* value was within ± 0.05 of the standard. For example, the detection of *N*-palmitoyldopamine in the first instar larvae can be seen in Figure 3. All the retention times and *m/z* values for the fatty acid amides detected in each instar and the

pure, standard compounds are in supplementary materials (Tables S2-S8). Any fatty acid amide characterized/quantified from the extract from each instar is listed in Table 4.

The scatter in our instar abundance data for fatty acid amides precludes definitive conclusions. The scatter in our data is not unusual. Tortoriello *et al*. [26] report that a series of fatty acid amides are found in *D. melanogaster* with some of their data exhibiting scatter similar to what we report here. Comparable levels of scatter are found in the values reported for the human plasma levels of the *N*-acylethanolamines [55]. Marchioni *et al*. [24] reviewed the LC-MS methods and challenges in measuring the "sub-trace" levels of the endocannabinoids in biological samples. The data included in the review from Marchioni *et al*. [24] often scatter like that shown in Table 4. The scatter in our data likely results from the low abundance of the fatty acid amide, averaging the values across the multiday instars, averaging the values from the complete body of the silkworm, and combining data between male and female *B. mori*. Fatty acid amide profiles from a single tissue or regions within a single tissue generally show less scatter [56,57].

Despite the scatter in our data, some trends do emerge. The set of fatty acid amides identified in a life cycle stage is unique to that stage; the pattern of fatty acid amides differs from stage-to-stage. None of the fatty acid amides we detected were found in every life cycle stage of *B. mori*. The closest was *N*-palmitoylglycine which was detected in all life cycle stages except instar 4. These results suggest the fatty acid amides have specialized functions in *B. mori* and are produced only when needed. The data for oleamide stands out from this perspective because oleamide could only be detected in two instars, instar 3 and instar 5, and was the most abundant of all the fatty acid amides we could detect and quantify, 660 ± 140 pmoles/g tissue in instar 3. The amount of oleamide found in instar 3 represents ~60% of the total amount of all the fatty acids we quantified across the life cycle of *B. mori*, 1100 pmoles/g tissue. Clearly, oleamide is most important to *B. mori* in instar 3.

Furthermore, our results show the fatty acid amides, as a class, are most abundant during instar 3 and instar 4. Including oleamide, the fatty acid amide levels in instar 3 and instar 4 represent 70-80% of the sum total of all the fatty acid amides found across the five instars, pupae, and moth. Even without including oleamide, the fatty acid amide levels in instar 3 and instar 4 represent 60-70% of the sum total of all the non-oleamide fatty acid amides found across the life cycle of *B. mori*. *In vitro* substrate specificity studies show only *Bm*-iAANAT, of the three known iAANATs expressed by *B. mori*, will accept long-chain acyl-CoAs required for the production of the fatty acid amides. We found appreciable levels of *Bm*-iAANAT expression in instar 3 and instar 4 consistent with the abundance of the fatty acid amides in these life cycle stages. A comparison of expression data for the three *Bm*-iAANATs to fatty acid amide data highlights the difficulty in assigning *in vivo* substrate specificity based on *in vitro* substrate specificity. Saghatelian *et al*. [58] found a relatively poor correlation between *in vitro* substrate specificity data for fatty acid amide hydrolase (FAAH) compared to the fatty acid amides that accumulated in FAAH (-/-) mice. We found comparable levels of *Bm*-iAANAT expression across of the life cycle stages of *B. mori*, yet the fatty acid amides were most abundant in instar 3 and 4.

4. Conclusion

One goal of this work was to identify a match between the published *in vitro* substrate specificity data for *Bm*-iAANAT and *Bm*-iAANAT3 and our results on the levels of the fatty acid amides and *Bm*-iAANAT transcripts at the different life cycle stages of *B. mori*. Correlations of these three data sets will provide insight about the potential involvement of the *Bm*-iAANATs in the biosynthesis of the fatty acid amides. Transcript levels for *Bm*-iAANAT3 are highest in instar 1, a life cycle stage exhibiting only a few fatty acid amides of low abundance. It seems unlikely *Bm*-iAANAT3 has a significant role in fatty acid amide biosynthesis; a hypothesis consistent with *in vitro* studies demonstrating that *Bm*-iAANAT3 prefers short-chain acyl-CoA substrates [40]. Most likely, the *Bm*-iAANAT3-catalyzed acetylation of specific amines is most important to *B. mori* during instar 1.

Transcript levels for *Bm*-iAANAT are found throughout all the life cycle stages with relatively little variation. Measurable levels for the *Bm*-iAANAT2 transcript were found throughout all the life cycle stages of *B. mori*, but with higher levels in instar 1 and instar 5. These data suggest that the reactions catalyzed by *Bm*-iAANAT and *Bm*-iAANAT2 have a role in each stage of *B. mori* life, meaning that *Bm*-iAANAT and *Bm*-iAANAT2 both have a "general purpose" or "house-keeping" role for *B. mori*. *Bm*-iAANAT will accept long-chain acyl-CoA thioesters as substrates [28]; thus, it seems likely that *Bm*-iAANAT does contribute to fatty acid amide biosynthesis *in vivo*. However, fatty acid amides and transcripts for *Bm*-iAANAT2 are found in every life cycle stage, suggesting that *Bm*-iAANAT2, like *Bm*-AANAT, does contribute to fatty acid amide biosynthesis in *B. mori*.

While our data do not ascribe function(s) to specific fatty amides or to the three *Bm*-iAANATs, our data do provide a "road-map" for future work to identify functions for these biomolecules. We found the fatty acid amides to be most abundant in instar 3 and instar 4, suggesting research to define fatty acid amide function should be focused on these life cycle stages. Future work to knock-down expression of individual *Bm*-iAANATs should focus on behavioral changes in instars 1, 3, and 4 and could be coupled to metabolomic studies to identify any changes in the

fatty acid amidome. We have used this subtraction metabolomic approach to provide evidence that peptidylglycine α-amidating monooxygenase [59], glycine *N*-acyltransferase-like 3 [59], and arylalkylamine *N*-acetyltransferase-like-2 [34] are involved in the cellular production of specific fatty acid amides.

Acknowledgements

This work has been supported by grants from the University of South Florida (a Proposal Enhancement grant), the Shirley W. and William L. Griffin Charitable Foundation, the National Institute of Drug Abuse at the National Institutes of Health (R03-DA034323), and the National Institute of General Medical Science at the National Institutes of Health (R15-GM107864) to D.J.M. This work has also received support from the Mass Spectrometry and Peptide Facility, Department of Chemistry, University of South Florida.

References

1. Soumya, M., Harinatha Reddy, A., Nageswari, G., and Venkatappa, B. (2017) Silkworm (*Bombyx mori*) and Its Constituents: a Fascinating Insect in Science and Research. *J. Entomol. Zool. Stud*. **5**, 1701-1705.
2. Businesswire, www.businesswire.com/news/home/20200629005608/en/Outlook-World-Silk-Market-2020-2027-Potential-Impac
3. International Sericultural Commission, www.inserco.org
4. Kaito, C., Akimitsu, N., Watanabe, H., and Sekimizu, K. (2002) Silkworm Larvae as an Animal Model of Bacterial Infection Pathogenic to Humans. M*icrob. Pathog.* **32,** 183-190. (DOI: 10.1006/mpat.2002.0494)
5. Hamamoto, H., Tonoike, A., Narushima, K., Horie, R., and Sekimizu, K. (2009) Silkworm as a Model Animal to Evaluate Drug Candidate Toxicity and Metabolism. *Comp. Biochem. Physiol. C Toxicol. Pharmacol.* **149**, 334–339 (DOI: 10.1016/j.cbpc.2008.08.008)
6. Meng, X., Zhu, F., and Chen, K. (2017) Silkworm: A Promising Model Organism in Life Science. *J. Insect Sci*. **17**, 1-6. (DOI: 10.1093/jisesa/iex064)
7. Ma, S.-Y., Smagghe, G., and Xia, Q.-Y. (2019) Genome Editing in *Bombyx mori*: New Opportunities for Silkworm Functional Genomics and the Sericulture Industry. *Insect Sci*. **26**, 964–972. (DOI 10.1111/1744-7917.12609)
8. Reis, U., Blum, B., von Specht, B.-U., Domdey, H., and Collins, J. (1992) Antibody Production in Silkworm Cells and Silkworm Larvae Infected with a Dual Recombinant *Bombyx mori* Nuclear Polyhedrosis Virus. *Biotechnology (NY)* **10**, 910-912 (DOI: 10.1038/nbt0892-910).
9. Yao, L., Wang, S., Su, S., Yao, N., He, J., Peng, L., and Sun, J. (2012) Construction of a Baculovirus-Silkworm Multigene Expression System and Its Application on Producing Virus-Like Particles. *PLoS One* **7**, e32510. (DOI: 10.1371/journal.pone.0032510)
10. Paul, D., and Dey S. (2014) Essential Amino acids, Lipid Profile and Fat-Soluble Vitamins of the Edible Silkworm *Bombyx mori* (Lepidoptera: Bombycidae). *Int. J. Trop. Insect Sci.* **34**, 239-247. (DOI: 10.1017/S1742758414000526)
11. Nongonierma, A.B., and FitzGerald, R.J. (2017) Unlocking the Biological Potential of Proteins from Edible Insects through Enzymatic Hydrolysis: A Review. *Innov. Food Sci. Emerg. Technol*. **43**, 239-252. (DOI: 10.1016/j.ifset.2017.08.014)
12. Farrell, E.K., and Merkler, D. J. (2008) Biosynthesis, Degradation and Pharmacological Importance of the Fatty Acid Amides. *Drug Discov. Today* **13**, 558-568. (DOI: 10.1016/j.drudis.2008.02.006)
13. Fezza, F., Bari, M., Florio, R., Talamonti, E., Feole, M., and Maccarrone, M. (2014) Endocannabinoids, Related Compounds and Their Metabolic Routes. *Molecules* **19**, 17078-17106. (DOI: 10.3390/molecules191117078)
14. Iannotti, F.A., Di Marzo, V., and Petrosino, S. (2016) Endocannabinoids and Endocannabinoid-related Mediators: Targets, Metabolism and Role in Neurological Disorders. *Prog. Lipid Res*. **62**, 107-128. (DOI: 10.1016/j.plipres.2016.02.002)
15. Bradshaw, H.B., Lee, S.H., and McHugh, D. (2009) Orphan Endogenous Lipids and Orphan GPCRs: A Good Match. *Prostaglandins Other Lipid Mediat*. **89**, 131-134. (DOI: 10.1016/j.prostaglandins.2009.04.006)
16. Devane, W.A., Hanuš, L., Breuer, A., Pertwee, R.G., Stevenson, L.A., Griffin, G., Gibson, D., Mandelbaum, A., Etinger, A., and Mechoulam, R. (1992) Isolation and Structure of a Brain Constituent that Binds to the Cannabinoid Receptor. *Science* **258**, 1946–1949. (DOI: 10.1126/science.1470919)
17. Showalter, V.M., Compton, D.R., Martin, B.R., and Abood, M.E. (1996) Evaluation of Binding in a Transfected Cell Line Expressing a Peripheral Cannabinoid Receptor (CB_2): Identification of Cannabinoid Receptor Subtype Selective Ligands. *J. Pharmacol. Exp. Ther*. **278**, 989-999.
18. Petrosino, S., and Di Marzo, V. (2017) The Pharmacology of Palmitoylethanolamide and First Data on the Therapeutic Efficacy of Some of Its New Formulations. *Br. J. Pharmacol*. **174**, 1349-1365. (DOI: 10.1111/bph.13580)

19. Cravatt, B.F., Prospero-Garcia, O., Siuzdak, G., Gilula, N.B., Henriksen, S.J., Boger, D.L., and Lerner, R.A. (1995) Chemical Characterization of a Family of Brain Lipids that Induce Sleep. *Science* **268**, 1506-1509. (DOI: 10.1126/science.7770779)
20. Alborn, H.T., Turlings, T.C.J., Jones, T.H., Stenhagen, G., Loughrin, J.H., and Tumlinson, J.H. (1997) An Elicitor of Plant Volatiles from Beet Armyworm Oral Secretion. *Science* **276**, 945–949. (DOI: 10.1126/science.276.5314.945)
21. Yoshinaga, N. (2016) Physiological Function and Ecological Aspects of Fatty Acid-Amino Acid Conjugates in Insects. *Biosci. Biotechnol. Biochem*. **80**, 1274-1282. (DOI: 10.1080/09168451.2016.1153956)
22. Bisogno, T., Sepe, N., De Petrocellis, L., Mechoulam, R., and Di Marzo, V. (1997) The Sleep Inducing Factor Oleamide is Produced by Neuroblastoma Cells. *Biochem. Biophys. Res. Commun*. **239**, 473-479. (DOI: 10.1006/bbrc.1997.7431)
23. Bradshaw, H.B., Rimmerman, N., Hu, S. S.-J., Burstein, S., and Walker, J.M. (2009) Novel Endogenous *N*-Acyl Glycines: Identification and Characterization. *Vitam. Horm*. **81**, 191-205. (DOI: 10.1016/S0083-6729(09)81008-X)
24. Marchioni, C., de Souza, I.D., Junior, V.R.A., de Souza Crippa, J.A., Tumas, V., and Queiroz, M.E.C. (2018) Recent Advances in LC-MS/MS Methods to Determine Endocannabinoids in Biological Samples: Application in Neurodegenerative Diseases. *Anal. Chim. Acta* **1044**, 12-28. (DOI: 10.1016/j.aca.2018.06.016)
25. Fezza, F., Dillwith, J.W., Bisogno, T., Tucker, J.S., Di Marzo, V., and Sauer, J.R. (2003) Endocannabinoids and Related Fatty Acid Amides, and Their Regulation in the Salivary Glands of the Lone Star Tick. *Biochim. Biophys. Acta* **1633**, 61-67. (DOI: 10.1016/s1388-1981(03)00087-8)
26. Tortoriello, G., Rhodes, B.P., Takacs, S.M., Stuart, J.M., Basnet, A., Raboune, S., Widlanski, T.S., Doherty, P., Harkany, T., and Bradshaw, H.B. (2013) Targeted Lipidomics in *Drosophila melanogaster* Identifies Novel 2-Monoacylglycerols and *N*-Acyl Amides. *PLoS One* **8**, e67865. (DOI: 10.1371/journal.pone.0067865)
27. Jeffries, K.A., Dempsey, D.R., Behari, A.L., Anderson, R.L., and Merkler, D.J. (2014) *Drosophila melanogaster* as a Model System to Study Long-chain Fatty Acid Amide Metabolism. *FEBS Lett.* **588**, 1596-1602. (DOI: 10.1016/j.febslet.2014.02.051)
28. Anderson, R.L., Battistini, M.R., Wallis, D.J., Shoji, C., O'Flynn, B.G., Dillashaw, J.E., and Merkler, D.J. (2018) *Bm*-iAANAT and Its Potential Role in Fatty Acid Amide Biosynthesis in *Bombyx mori*. *Prostaglandins, Leuokot. Essent. Fatty Acids* **135**, 10-17. (DOI: 10.1016/j.plefa.2018.06.001)
29. Tsuboi, K., Uyama, T., Okamoto, Y., and Ueda, N. (2018) Endocannbinoids and Related *N*-Acylethanolamines: Biological Activities and Metabolism. *Inflamm. Regen*. **38**, 28. (DOI:10.1186/s41232-018-0086-5)
30. Merkler, D.J., Merkler, K.A., Stern, W., and Fleming, F.F. (1996) Fatty Acid Amide Biosynthesis: A Possible New Role for Peptidylglycine α-Amidating Enzyme and Acyl-Coenzyme A:Glycine *N*-Acyltransferase. *Arch. Biochem. Biophys*. **330**, 430-434 (DOI: 10.1006/abbi.1996.0272)
31. Vetting, M.W., de Carvalho, L.P.S., Yu, M., Hegde, S.S., Magnet, S., Roderick, S.L., and Blanchard, J.S. (2005) Structure and Functions of the GNAT Superfamily of Acetyltransferases. *Arch. Biochem. Biophys*. **433**, 212-226 (DOI: 10.1016/j.abb.2004.09.003)
32. Ud-Din, A.I.M.S., Tikhomirova, A., and Roujeinikova, A. (2016) Structure and Functional Diversity of GCN5-Related *N*-Acetyltransferases, *Int. J. Mol. Sci*. **17**, 1018. (DOI: 10.3390/ijms17071018)
33. Dempsey, D.R., Jeffries, K.A., Anderson, R.L., Carpenter, A.-M., Rodriguez Ospina, S., and Merkler, D.J. (2014) Identification of an Arylalkylamine *N*-Acyltransferase from *Drosophila melanogaster* that Catalyzes the Formation of Long-chain *N*-Acylserotonins. *FEBS Lett*. **588**, 594-599. (DOI: 10.1016/j.febslet.2013.12.027)
34. Anderson, R.L., Wallis, D.J., Aguirre, A., Holliday, D., and Merkler, D.J. (2019) Knockdown of Arylalkylamine *N*-Acetyltransferase-like 2 in *Drosophila melanogaster*. *Arch. Insect Biochem. Physiol*. **102**, e21608. (DOI: 10.1002/arch.21608)
35. McPartland, J.M., Agraval, J., Gleeson, D., Heasman, K., and Glass, M. (2006) Cannabinoid Receptors in Invertebrates. *J. Evol. Biol*. **19**, 366-373. (DOI: 10.1111/j.1420-9101.2005.01028.x)
36. Han, Q., Robinson, H., Ding, H., Christensen, B.M., and Li, J. (2012) Evolution of Insect Arylalkylamine N-Acetyltransferases: Structural Evidence from the Yellow Fever Mosquito, Aedes aegypti. Proc. Natl. Acad. Sci. USA **109**, 11669-11674. (DOI: 10.1073/pnas.1206828109)
37. Hiragaki, S., Suzuki, T., Mohamed, A.A.M., and Takeda, M. (2015) Structures and Functions of Insect Arylalkylamine *N*-Acetyltransferase (iaaNAT); a Key Enzyme for Physiological and Behavior Swith in Arthropods. *Front. Physiol*. **6**, 113 (DOI:10.3389/fphys.2015.00113)
38. Tsugehara, T., Iwai, S., Fujiwara, Y., Mita, K., and Takeda, M. (2007) Cloning and Characterization of Insect Arylalkylamine *N*-Acetyltransferase from *Bombyx mori*. *Comp. Biochem. Physiol. B Biochem. Mol. Biol*. **147**, 358-366. (DOI: 10.1016/j.cbpb.2006.10.112)

39. Long, Y., Li, J., Zhao, T., Li, G., and Zhu, Y. (2015) A New Arylalkylamine *N*-Acetransferase in Silkworm (*Bombyx mori*) Affects Integument Pigmentation. *Appl. Biochem. Biotechnol*. **175**, 3447-3457. (DOI: 10.1007/s12010-015-1516-3)
40. Battistini, M.R., O'Flynn, B.G., Shoji, C., Suarez, G., Galloway, L.C., and Merkler, D.J. (2019) *Bm*-iAANAT3: Expression and Characterization of a Novel Arylalkylamine *N*-acyltransferase from *Bombyx mori*. *Arch. Biochem. Biophys*. **661**, 107-116. (DOI: 10.1016/j.abb.2018.11.015)
41. Hachouf-Gherras, S., Besson, T., and Bosquet, G. (1998) Identification and Developmental Expression of a *Bombyx mori α-Tubulin* Gene. *Gene* **208**, 89-94. (DOI: 10.1016/S0378-1119(97)00660-4)
42. Nie, Z., Lü, P., Chen, X., Wang, Q., Meng, X., Lu, S., and Chen, K. (2017) Reference Gene Selection for Quantitative Real-time Polymerase Chain Reaction Analysis in Bombyx mori Nucleopolyhedrovirus-infected Silkworms. *Invertebr. Surviv. J.* **14**, 94-102. (DOI: 10.25431/1824-307X/isj.v14i1.94-102)
43. Peng, R., Zhai, Y., Ding, H., Di, T., Zhang, T., Li, B., Shen, W., and Wei, Z. (2012) Analysis of Reference Gene Expression for Real-time PCR Based on Relative Quantitation and Dual Spike-in Strategy in the Silkworm *Bombyx mori*. *Acta Biochim Biophys Sin. (Shanghai)* **44,** 614-622. (DOI: 10.1093/abbs/gms040)
44. Heid, C.A., Stevens, J., Livak, K.J., and Williams, P.M. (1996) Real Time Quantitative PCR. *Genome Res*. **6**, 986-944. (DOI:10.1101/gr.6.10.986)
45. O'Flynn, B.G., Suarez, G., Hawley, A.J., and Merkler, D.J. (2018) Insect Arylalkylamine *N*-Acyltransferases: Mechanism and Role in Fatty Acid Amide Biosynthesis. *Front. Mol. Biosci*. **5**, 66. (DOI: 10.3389/fmolb.2018.00066).
46. Dai, F.-y., Qiao, L., Tong, X.-l., Cao, C., Chen, P., Chen, J., Lu, C., and Xiang, Z.-h. (2010) Mutations of an Arylalkylamine-*N*-Acetyltransferase, Bm-iAANAT, are Responsible for Silkworm Melanism Mutant. *J. Biol. Chem*. **285**, 19553-19560. (DOI: 10.074/jbc.M109.096743)
47. Itoh, M.T., Hattori, A., Nomura, T., Sumi, Y., and Suzuki, T. (1995) Melatonin and Arylalkylamine *N*-Acetyltransferase Activity in the Silkworm, *Bombyx mori*. *Mol. Cell. Endocrinol*. **115**, 59-64. (DOI: 10.1016/0303-7207(95)03670-3)
48. Zhan, S., Guo, Q., Li, M., Li, M., Li, J., Miao, X., and Huang, Y. (2010) Disruption of an N-Acetyltransferase Gene in the Silkworm Reveals a Novel Role in Pigmentation. *Development* **137**, 4083-4090. (DOI: 10.1242/dev.053678)
49. Takeda, S. (2003) *Bombyx mori*. ***In***: Encyclopedia of Insects, Resh, V.H., and Cardé, R.T. (Eds.), pp. 133-135, Elsevier Science & Technology, San Diego.
50. Tsujita, M., and Sakurai, S. (1971) Genetic and Biochemical Studies of the Lethal Albino Larvae of the Silkworm. *Bombyx mori*. *Jpn. J. Genet*. **46**, 17-31. (DOI: 10.1266/jjg.46.17)
51. Reddy, B.V., Divya, P., and Anitha, M. (2015) Quantitative Profile Analysis of Mulberry Silkworm *Bombyx mori L* (CSR2XCSR4). *Int. Lett. Nat. Sci*. **34**, 34-41 (DOI: 10.18052/www.scipress.com/ILNS.34.34)
52. Wang, M.-x., Cai, Z.-z., Lu, Y., Xin, H.-H., Chen, R.-t., Liang, S., Singh, C.O., Kim, J.-N., Niu, Y-s., and Miao, Y.-g. (2013) Expression and Functions of Dopa Decarboxylase in the Silkworm, Bombyx mori was Regulated by Molting Hormone. *Mol. Biol. Rep*. **40**, 4415-4122. (DOI: 10.1007/s11033-013-2514-6)
53. Aso, Y., Nakashima, K., and Yamasaki, N. (1990) Changes in the Activity of Dopa Quinone Imine Conversion Factor During the Development of *Bombyx mori*. *Insect Biochem*. **20**, 685-689. (DOI: 10.1016/0020-1790(90)90082-6)
54. Liu, Y., Beyer, A., and Aebersold, R. (2016) On the Dependency of Cellular Protein Levels on mRNA Abundance. *Cell* **165**, 535-550. (DOI: 10.1016/j.cell.2016.03.014)
55. Balvers, M.G.J., Wortelboer. H.M., Witkamp, R.F., and Verhoeckx, K.C.M. (2013) Liquid Chromatgraphy-Tandem Mass Spectrometry Analysis of Free and Esterified Fatty Acid *N*-Acyl Ethanolamines in Plasma and Blood Cells. *Anal. Biochem*. **434**, 275-283. (DOI: 10.1016/j.ab.2012.11.008)
56. Richardson, D., Ortori, C.A., Chapman, V., Kendall, D.A., and Barrett, D.A. (2007) Quantitative Profiling of Endocannabinoids and Related Compounds in Rat Brain using Liquid Chromatography-Tandem Electrospray Ionization Mass Spectrometry. *Anal. Biochem*. **360**, 216-226. (DOI: 10.1016/j.ab.2006.10.039)
57. Chotiwon, N., Andre, B.G., Sanchez-Vargas, I., Islam, M.N., Grabowski, J.M., Hopf-Jannasch, A., Gough, E., Nakayasu, E., Blair, C.D., Belisle, J.T., Hill, C.A., Kuhn, R.J., and Perera, R. (2018) Dynamic Remodeling of Lipids Coincides with Dengue Virus Replication in the Midgut of *Aedes aegypti* Mosquitoes. *PLoS Pathog.* **14**, e1006853. (DOI: 10.1371/journal.ppat.1006853)
58. Saghatelian, A., McKinney, M.K., Bandell, M., Patapoutian, A., and Cravatt, B.F. (2004) A FAAH-Regulated Class of *N*-Acyl Taurines That Activates TRP Ion Channels. *Biochemistry* **45**, 9007-9015. (DOI: 10.1021/bi0608008)
59. Jeffries, K.A., Dempsey, D.R., Farrell, E.K., Anderson, R.L., Garbade, G.J., Gurina, T.S., Gruhonjic, I., Gunderson, C.A., and Merkler, D.J. (2016) Glycine *N*-Acyltransferase-like 3 is Responsible for Long-chain *N*-Acylglycine Formation in $N_{18}TG_2$ Cells. *J. Lipid Res*. **57**, 781-790. (DOI: 10.1194/jlr.M062042)

Figure Legends

Figure 1. The Reaction Catalyzed by the *Bm*-iAANATs. Substrate specificities to define R and R1 have been described for *Bm*-iAANAT (28), *Bm*-iAANAT2 (28), and *Bm*-iAANAT3 (40).

Figure 2. Relative Transcript Levels of *Bm*-iAANAT, *Bm*-iAANAT2, *Bm*-iAANAT3 from the Life Cycle Stages of *Bombyx mori*. All relative expression values are fold changes calculated using $2^{-\Delta\Delta CT}$. The fold changes for instar 1 are represented by 1.00 to denote the baseline of AANAT transcript abundance at the earliest life stage used in these experiments.

Figure 3. Identification of *N*-Palmitoyldopamine in *Bombyx mori* from First Instar Larvae. The retention time and *m/z* values of the commercial standard of *N*-palmitoyldopamine (panels A and B respectively) closely match the retention time and *m/z* values for the endogenous *N*-palmitoyldopamine isolated from *B.mori* first instar larvae (panels C and D respectively).

Table 1

Decontamination of gDNA from mRNA isolations

Reagent	**Recommended Protocol[a]**	**Modified Protocol**
mRNA	1 µg	1 µg
DNase I	1 µL	2 µL
DNase I Buffer with $MgCl_2$	1 µL	2 µL
Nuclease-Free Water	to 10 µL	to 18 µL

[a]As recommended by the manufacturer.

Table 2

RT-qPCR Forward and Reverse Primers for Tua1, *Bm*-iAANAT, *Bm*-iAANAT2, and *Bm*-iAANAT3

Amplicon	Forward Primer	Reverse Primer
Tua1	AGATGCCCACAGACAAGACC	CAAGATCGACGAAGAGAGCA
Bm-iAANAT	CAAAATGTCCGTTCCAGCTT	GATTGACGGCGAGATTCATT
Bm-iAANAT2	GAACGAGGCAGTAGGGTTATATG	CCTTTCAGTAGCGAATCCCTG
Bm-iAANAT3	CCTTAGAACGTCTTTGCCTCG	TCGGTGGACTGCTTTATCTTC

Table 3

ΔC_T values for *Bm*-iAANAT, *Bm*-iAANAT2 and *Bm*-iAANAT3 in each Life Stage of *Bombyx mori*.

Amplicon	**Instar 1 (ΔC_T)**	**Instar 2 (ΔC_T)**	**Instar 3 (ΔC_T)**	**Instar 4 (ΔC_T)**	**Instar 5 (ΔC_T)**	**Pupae (ΔC_T)**	**Moth (ΔC_T)**
***Bm*-iAANAT**	2.75 ± 0.08	4.55 ± 0.35	2.54 ± 0.45	3.72 ± 0.11	1.70 ± 0.17	3.54 ± 0.28	2.05 ± 0.24
***Bm*-iAANAT2**	2.37 ± 0.07	5.23 ± 0.34	4.50 ± 0.43	5.18 ± 0.19	2.80 ± 0.22	5.39 ± 0.25	4.98 ± 0.10
***Bm*-iAANAT3**	5.25 ± 0.11	11.85 ± 0.34	12.84 ± 0.60	12.99 ± 0.23	12.79 ± 0.22	10.19 ± 0.23	13.53 ± 0.17

Table 4

Quantification of Fatty Acid Amides Detected in Different Life Stages of *Bombyx mori*[a]

	pmoles/g						
Fatty Acid Amide	**Instar 1**	**Instar 2**	**Instar 3**	**Instar 4**	**Instar 5**	**Pupae**	**Moth**
PalmGly	2.88 ± 0.92	11.3 ± 2.3	15.3 ± 0.40	N.D.	5.68 ± 1.3	2.08 ± 0.12	3.69 ± 1.5
PalmDop	5.46 ± 0.54	2.77 ± 1.1	N.D.	N.D.	1.12 ± 0.13	0.606 ± 0.29	N.D.
PalmSer	N.D.	N.D.	N.D.	9.85 ± 0.62	N.D.	0.927 ± 0.12	6.04 ± 4.4
Palmle	N.D.	N.D.	6.45 ± 1.2	21.6 ± 13	1.06 ± 0.32	N.D.	N.D.
Palm	N.D.	N.D.	21.8 ± 8.7	27.5 ± 19	N.D.	N.D.	N.D.
OleGly	N.D.	29.7 ± 11	N.D.	N.D.	31.9 ± 25	N.D.	N.D.
OleEth	1.62 ± 0.45	N.D.	2.48 ± 0.68	19.9 ± 15	4.52 ± 1.3	N.D.	0.225 ± 0.13
OleDop	1.74 ± 1.0	N.D.	6.96 ± 5.5	5.96 ± 0.29	N.D.	2.97 ± 2.5	N.D.
OleSer	N.D.	N.D.	3.03 ± 0.81	3.51 ± 0.61	N.D.	N.D.	N.D.
OleTrp	1.90 ± 0.24	N.D.	N.D.	N.D.	N.D.	0.431 ± 0.10	N.D.
Ole	N.D.	N.D.	661 ± 135	N.D.	119 ± 93	N.D.	N.D.
AracSer	N.D.	N.D.	N.D.	13.8 ± 2.9	N.D.	N.D.	0.924 ± 0.66
LinGly	N.D.	N.D.	28.2 ± 7.2	N.D.	N.D.	N.D.	N.D.
Lino	N.D.	N.D.	9.23 ± 1.6	22.1 ± 14	N.D.	N.D.	N.D.
SteSer	N.D.	N.D.	N.D.	N.D.	N.D.	0.503 ± 0.10	6.06 ± 2.7

[a]N.D. = not detected

Figure 1

The Reaction Catalyzed by the *Bm*-iAANATs.

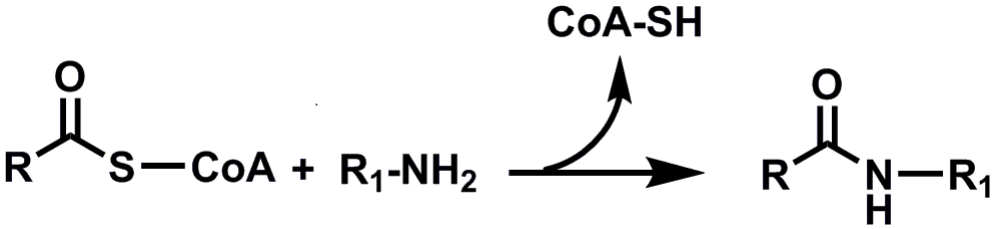

Figure 2

Relative Transcript Levels of *Bm*-iAANAT, *Bm*-iAANAT2, *Bm*-iAANAT3 from the Life Cycle Stages of *Bombyx mori*.

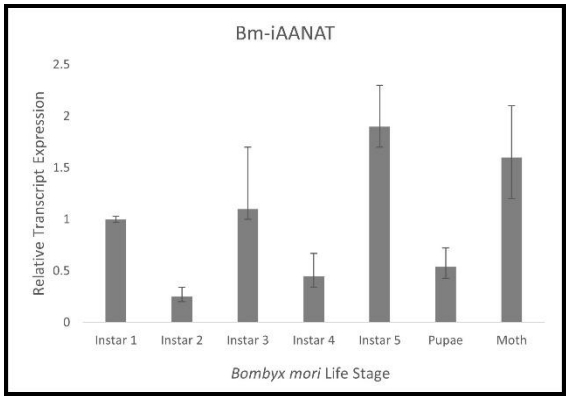

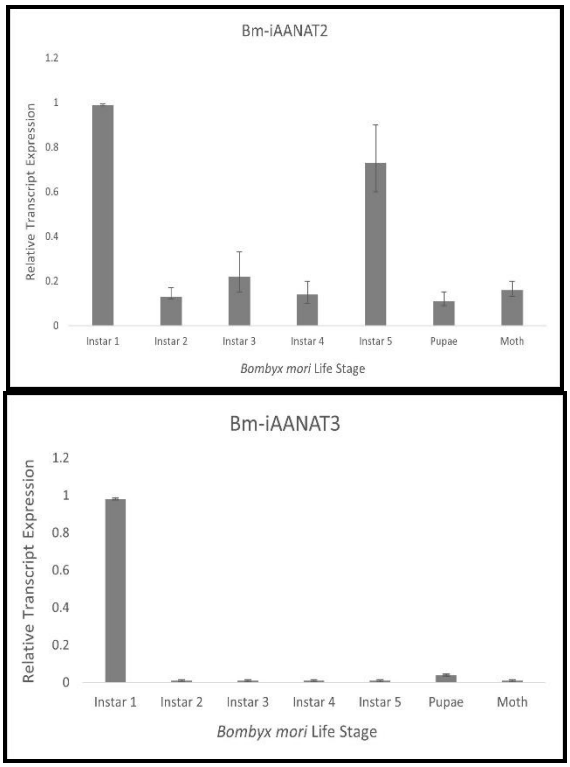

Figure 3

Identification of *N*-Palmitoyldopamine in *Bombyx mori* from First Instar Larvae.

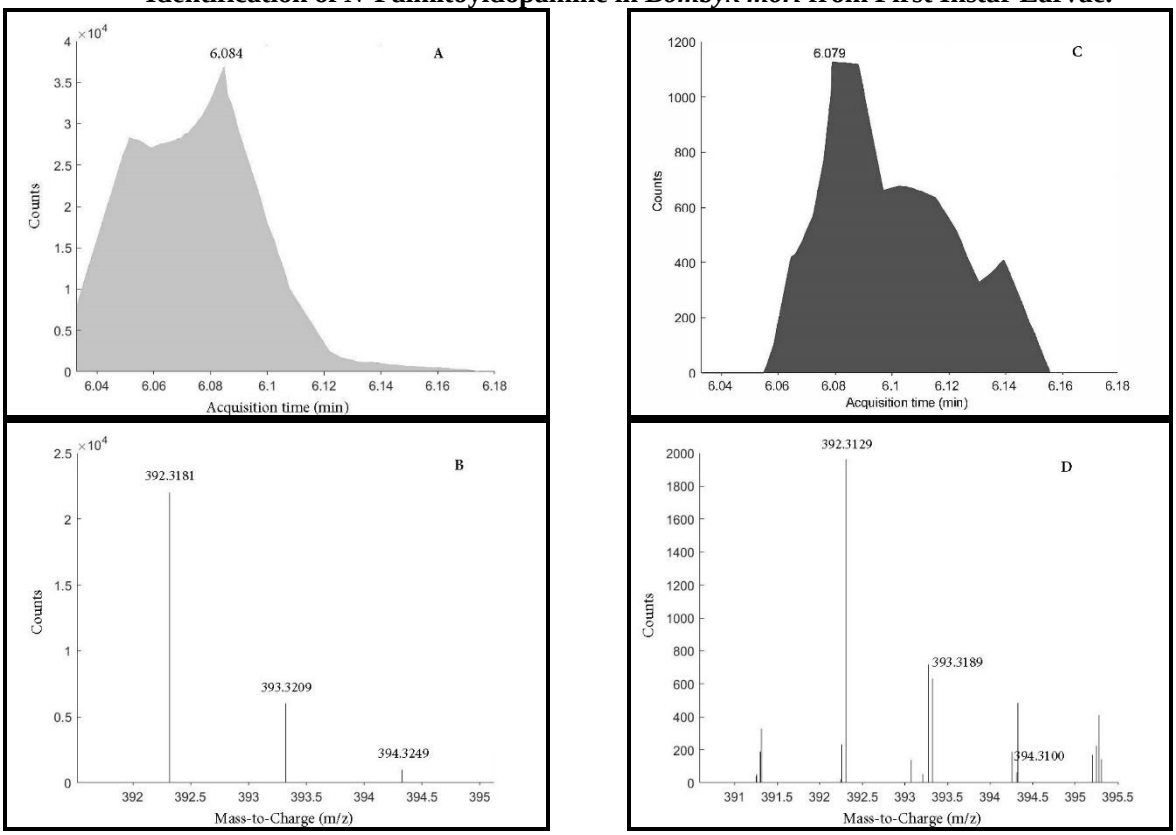

Table S1

C_T values for Tua1, *Bm*-iAANAT, *Bm*-iAANAT2 and *Bm*-iAANAT3 in each Life Stage of *Bombyx mori*.

Amplicon	**Instar 1 (CT)**	**Instar 2 (CT)**	**Instar 3 (CT)**	**Instar 4 (CT)**	**Instar 5 (CT)**	**Pupae (CT)**	**Moth (CT)**
TUA 1	16.48 ± 0.06	14.25 ± 0.32	17.56 ± 0.43	14.80 ± 0.07	17.86 ± 0.15	15.28 ± 0.22	14.31 ± 0.10
***Bm*-iAANAT**	19.23 ± 0.06	18.80 ± 0.16	20.10 ± 0.12	18.52 ± 0.09	19.56 ± 0.08	18.82 ± 0.17	16.36 ± 0.22
***Bm*-iAANAT2**	18.85 ± 0.04	19.48 ± 0.14	22.06 ± 0.03	19.98 ± 0.18	20.66 ± 0.16	20.67 ± 0.12	19.29 ± 0.04
***Bm*-iAANAT3**	21.73 ± 0.09	26.10 ± 0.12	30.40 ± 0.42	27.79 ± 0.22	30.65 ± 0.16	25.47 ± 0.06	27.84 ± 0.14

Table S2

Comparison of the Retention Times and *m/z* Values of *Bombyx mori* First Instar Larvae (*Bm*i1) and the Pure Standards used for Detection

Fatty Acid Amide	*m/z*		Retention Time (min)	
	Standard	*Bm*i1	Standard	*Bm*i1
N-Palmitoyldopamine	392.3181	392.3129	6.084	6.079
N-Palmitoylglycine	314.2709	314.2675	5.917	5.912
Palmitamide	256.2593	256.2569	6.184	6.181
N-Oleoyldopamine	418.32547	418.3194	6.200	6.204
N-Oleoylethanolamine	326.3002	326.2992	6.059	6.046
N-Oleoyltryptamine	425.3548	425.3691	6.583	6.577

Table S3

Comparison of the Retention Times and *m/z* Values of *Bombyx mori* Second Instar Larvae (*Bm*i2) and the Pure Standards used for Detection

Fatty Acid Amide	*m/z*		Retention Time (min)	
	Standard	*Bm*i2	Standard	*Bm*i2
N-Palmitoyldopamine	392.3177	392.3195	6.068	6.105
N-Palmitoylglycine	314.2701	314.2667	5.902	5.898
N-Oleoylglycine	340.2858	340.2844	5.993	5.839

Table S4

Comparison of the Retention Times and *m/z* Values of *Bombyx mori* Third Instar Larvae (*Bm*i3) and the Pure Standards used for Detection

Fatty Acid Amide	*m/z*		Retention Time (min)	
	Standard	*Bm*i3	Standard	*Bm*i3
N-Palmitoyldopamine	392.3095	392.3078	6.125	6.129
N-Palmitoylglycine	314.2639	314.2601	5.972	5.971
Palmitamide	256.2593	256.2569	6.184	6.181
Palmitoleamide	254.2438	254.2411	5.830	5.830
N-Oleoylethanolamine	326.3002	326.2992	6.059	6.046
N-Oleoyldopamine	418.3247	418.3194	6.200	6.204
N-Oleoylserotonin	441.3399	441.3142	6.229	6.295
Oleamide	282.2746	282.2715	6.254	6.254
N-Linoleoylglycine	338.2638	338.3091	5.806	5.797
Linoleamide	280.2590	280.2547	5.963	6.043

Table S5

Comparison of the Retention Times and *m/z* Values of *Bombyx mori* Fourth Instar Larvae (*Bm*i4) and the Pure Standards used for Detection

Fatty Acid Amide	*m/z*		Retention Time (min)	
	Standard	*Bm*i4	Standard	*Bm*i4
N-Palmitoylserotonin	415.3322	415.2882	6.187	6.125
Palmitamide	256.2645	256.2631	6.214	6.213
Palmitoleamide	254.2456	254.2463	5.837	5.859
N-Stearoylserotonin	443.3638	443.3505	6.542	6.576
N-Oleoyldopamine	418.3315	418.3306	6.248	6.246
N-Oleoylethanolamine	326.3057	326.3049	6.077	6.074
N-Oleoylglycine	340.2846	340.2847	6.094	5.945
N-Oleoylserotonin	441.3479	441.3483	6.262	6.322
Oleamide	282.2796	282.2786	6.289	6.277
Linoleamide	280.2643	280.2616	5.979	6.027
N-Arachidonoylserotonin	463.3326	463.3337	6.071	6.069

Table S6

Comparison of the Retention Times and *m/z* Values of *Bombyx mori* Fifth Instar Larvae (*Bm*i5) and the Pure Standards used for Detection

Fatty Acid Amide	*m/z*		Retention Time (min)	
	Standard	*Bm*i5	Standard	*Bm*i5
N-Palmitoyldopamine	392.3163	392.3153	6.065	5.951
N-Palmitoylglycine	314.2689	314.2975	5.899	6.001
Palmitoleamide	254.2482	254.2445	5.757	5.777
N-Oleoyldopamine	418.3316	418.3356	6.140	6.124
N-Oleoylethanolamine	326.3063	326.2927	5.982	5.986
N-Oleoylglycine	340.2848	340.3185	5.990	5.918
Oleamide	282.2794	282.2749	6.173	6.167

Table S7

Comparison of the Retention Times and *m/z* Values of *Bombyx mori* Pupae Larvae (*Bm*i-Pupae) and the Pure Standards used for Detection

Fatty Acid Amide	*m/z*		Retention Time (min)	
	Standard	*Bm*i-Pupae	Standard	*Bm*i-Pupae
N-Palmitoyldopamine	392.3157	392.3156	6.096	6.093
N-Palmitoylglycine	314.2681	314.2970	5.926	5.929
N-Palmitoylserotonin	415.3318	415.3221	6.125	6.074
N-Oleoyldopamine	418.3303	418.3292	6.167	6.161
N-Oleoyltryptamine	425.3523	425.3339	6.587	6.617
N-Stearoylserotonin	443.3626	443.3415	6.471	6.475

Table S8

Comparison of the Retention Times and *m/z* Values of *Bombyx mori* Moth Larvae (*Bm*i-Moth) and the Pure Standards used for Detection

Fatty Acid Amide	*m/z*		Retention Time (min)	
	Standard	*Bm*i-Moth	Standard	*Bm*i-Moth
N-Palmitoyldopamine	392.3168	392.3146	6.082	5.966
N-Palmitoylserotonin	415.3333	415.3558	6.115	6.087
N-Oleoylethanolamine	326.3071	326.3058	6.003	5.982
N-Arachidonoylserotonin	463.3299	463.3395	6.174	6.054
Linoleamide	280.2647	280.2633	5.908	5.896